

Universal conductance fluctuation of mesoscopic systems in the metal-insulator crossover regime

Zhenhua Qiao, Yanxia Xing, and Jian Wang*

Department of Physics and the Center of Theoretical and Computational Physics, The University of Hong Kong, Hong Kong, China

(Received 20 January 2010; published 22 February 2010)

We report a theoretical investigation on conductance fluctuation of mesoscopic systems. Extensive numerical simulations on quasi-one-dimensional, two-dimensional, and quantum dot systems with different symmetries [circular orthogonal ensemble, circular unitary ensemble (CUE), and circular symplectic ensemble (CSE)] indicate that the conductance fluctuation can reach a universal value in the crossover regime for systems with CUE and CSE symmetries. The conductance distribution is found to be a universal function from diffusive to localized regimes that depends only on the average conductance, dimensionality, and symmetry of the system. The numerical solution of DMPK equation agrees with our result in quasi-one dimension. Our numerical results in two dimensions suggest that this universal conductance fluctuation is related to the metal-insulator transition. In the localized regime with average conductance $\langle G \rangle < 0.3$, the conductance distribution seems to be superuniversal independent of dimensionality and symmetry.

DOI: 10.1103/PhysRevB.81.085114

PACS number(s): 72.15.Rn, 71.30.+h, 73.23.-b

I. INTRODUCTION

One of the most important features in mesoscopic system is that the conductance in the diffusive regime exhibits universal features with a universal conductance fluctuation (UCF) that depends only on the dimensionality and the symmetry of the system.¹ There exist three ensembles or symmetries according to the random matrix theory (RMT):² (1) circular orthogonal ensemble (COE) (characterized by symmetry index $\beta=1$) when the time-reversal and spin-rotation symmetries are present, (2) circular unitary ensemble (CUE) ($\beta=2$) if time-reversal symmetry is broken, and (3) circular symplectic ensemble (CSE) ($\beta=4$) if the spin-rotation symmetry is broken while time-reversal symmetry is maintained. In the diffusive regime, the UCF is given by $\text{rms}(G) = c_d / \sqrt{\beta} e^2 / h$, where $c_d = 0.73, 0.86, 0.70$ for quasi-one dimension (1D), two dimensions (2D), and quantum dot (QD) systems and $\beta = 1, 2, 4$.^{1,2} Although the RMT can apply to both diffusive and localized regimes, so far the universal conductance fluctuation has been addressed and established only in the diffusive regime. When the system is away from the diffusive regime, some universal behaviors have been observed. For instance, the conductance distribution of quasi-1D systems ($\beta=1$) with surface roughness was found to be universal in the crossover regime, independent of details of the system.³ For quasi-1D systems with $\beta=1, 2$, the conductance distribution obtained from tight-binding model agrees with the numerical solution of DMPK equation.⁴ In high dimensions, conductance distribution at the mobility edge of metal-insulator transition was also shown numerically to be universal for 2D systems with $\beta=2, 4$ and a 3D system with $\beta=1$.⁵ In the localized regime, the conductance distribution of 3D systems⁶ is qualitatively different from that of quasi-1D systems where the conductance distributions obey log-normal distribution.⁷ It would be interesting to further explore the universal behaviors of these systems and ask the following questions: Is there any universal behaviors away from mobility edge? Is it possible to have a UCF beyond the diffusive regime? If there is, what is the

nature of the UCF? It is the purpose of this work to investigate these issues.

To do this, we have carried out extensive numerical calculations for conductance fluctuations $\text{rms}(G)$ in quasi-1D, 2D, and QD *mesoscopic* systems for different symmetries $\beta=1, 2, 4$. Our results can be summarized as follows. (1) We confirmed that in the diffusive regime, the value of UCF is given by $\text{rms}(G) = c_d / \sqrt{\beta} e^2 / h$, where $c_d = 0.73, 0.86, 0.70$ for quasi-1D, 2D, and quantum dot systems. The conductance distribution in this regime was found to be Gaussian as expected. (2) From diffusive to localized regimes, the conductance distribution was found to be a universal function that depends only on the average conductance for quasi-1D, 2D, and QD *mesoscopic* systems and for $\beta=1, 2, 4$. (3) We found that there exists a second UCF in the crossover regime for $\beta=2, 4$ but not for $\beta=1$. Our results show that the UCF depends weakly on the symmetries of the system and assumes the following value: $\text{rms}(G) = \tilde{c}_d e^2 / h$. Here, for $\beta=2$, we found $\tilde{c}_d = 0.56 \pm 0.01, 0.68 \pm 0.01, 0.58 \pm 0.01$ for quasi-1D, 2D, and QD systems, respectively, while for $\beta=4$, we have $\tilde{c}_d = 0.55 \pm 0.01, 0.66 \pm 0.02, 0.56 \pm 0.01$. The conductance distribution in this regime was found to be one-sided log-normal in agreement with previous results.⁷ (4) For quasi-1D systems, the UCF occurs when the localization length ξ is approximately equal to the system size L , i.e., $\xi \sim L$ for $\beta=2, 4$. For 2D systems, we found that the occurrence of UCF is related to the metal-insulator transition. (5) In the localized regime with $\langle G \rangle < 0.3$, the conductance distribution does not seem to depend on dimensionality and symmetry. (6) For quasi-1D systems, the numerical solution of DMPK equation⁸ agrees with our results.

II. NUMERICAL RESULTS

A. Theoretical method

In the numerical calculations, we used the same tight-binding Hamiltonian as that of Ref. 9,

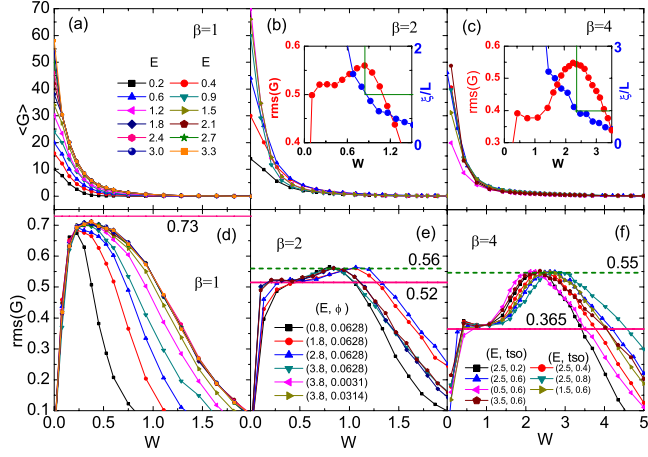


FIG. 1. (Color online) [(a)–(c)] Average conductance and [(d)–(f)] its fluctuation vs disorder strength W for different symmetry index β in quasi-1D systems. Insets: localization length vs W for $\beta=2, 4$.

$$\begin{aligned}
 H = & \sum_{nm\sigma} \epsilon_{nm} c_{nm\sigma}^\dagger c_{nm\sigma} - t \sum_{nm\sigma} \\
 & \times [c_{n+1,m\sigma}^\dagger c_{nm\sigma} e^{-im\phi} + c_{n,m-1\sigma}^\dagger c_{nm\sigma} + \text{H.c.}] - t_{so} \sum_{nm\sigma\sigma'} \\
 & \times [c_{n,m+1\sigma}^\dagger (i\sigma_x)_{\sigma\sigma'} c_{nm\sigma'} - c_{n+1,m\sigma}^\dagger (i\sigma_y)_{\sigma\sigma'} c_{nm\sigma'} e^{-im\phi} \\
 & + \text{H.c.}], \quad (1)
 \end{aligned}$$

where $c_{nm\sigma}^\dagger$ is the creation operator for an electron with spin σ on site (n, m) , $\epsilon_{nm\sigma} = 4t$ is the on-site energy, $t = \hbar^2/2\mu a^2$ is the hopping energy, and $t_{so} = \alpha_{so}/2a$ is the effective Rashba spin-orbit coupling. Here, the magnetic flux $\phi = \hbar\omega_c/2t$ and $\omega_c \equiv eB/\mu c$ is the cyclotron frequency. We choose $\mathbf{A} = (-By, 0, 0)$ so that the system has translational symmetry along x direction (from lead 1 to lead 3). Static Anderson-type disorder is added to the on-site energy with a uniform distribution in the interval $[-W/2, W/2]$, where W characterizes the strength of the disorder. The conductance G is calculated from the Landauer-Buttiker formula $G = (2e^2/h)T$, where the transmission coefficient T is given by $T = \text{Tr}(\Gamma_R G^r \Gamma_L G^a)$. Here, $G^{r,a}$ are the retarded and advanced Green's functions of central disordered region of the device which we evaluate numerically. The quantities $\Gamma_{L/R}$ are the line width functions describing coupling of the left or right leads to the scattering region. The conductance fluctuation is defined as $\text{rms}(G) \equiv \sqrt{\langle G^2 \rangle - \langle G \rangle^2}$, where $\langle \dots \rangle$ denotes averaging over an ensemble of samples with different disorder configurations of the same strength W . In the following, the average conductance and its fluctuation are measured in unit of e^2/h ; the magnetic field is measured using magnetic flux ϕ and t is used as the unit of energy.

B. Conductance fluctuation in quasi-one dimension

We first examine average conductances $\langle G \rangle$ and their fluctuations $\text{rms}(G)$ vs disorder strength W in quasi-1D systems with different symmetry index β (see Fig. 1). In our numerical simulation, the size of quasi-1D systems is chosen to be

40×2000 for $\beta=1, 2$ [Figs. 1(a) and 1(b)] and 40×800 for $\beta=4$ [Fig. 1(c)]. Each point in Fig. 1 is obtained by averaging 9000 configurations for $\beta=1$ and 15 000 configurations for $\beta=2, 4$. In Fig. 1, data with different parameters are shown. For instance, with $\beta=2$, $\langle G \rangle$ and $\text{rms}(G)$ vs W are plotted for different Fermi energies with fixed $\phi=0.0628$ and different magnetic flux with fixed Fermi energy $E=3.8$. From Fig. 1, we see that in the diffusive regime where $\langle G \rangle > 1$, there is a plateau region for $\text{rms}(G)$ with the plateau value approximately equal to the known UCF values $\text{rms}(G) = 0.73/\sqrt{\beta} = 0.73, 0.52, 0.365$ (marked by solid lines). This suggests that one way to identify UCF is to locate the plateau region in the plot of $\text{rms}(G)$ vs disorder strength and the plateau value should correspond to UCF. This method has been used to identify universal spin-Hall conductance fluctuation¹⁰ that was later confirmed by RMT.¹¹ Importantly, there exists a second plateau region for $\beta=2, 4$ but not for $\beta=1$. The plateau value approximately equals to $\text{rms}(G) = 0.56 \pm 0.01$ for $\beta=2$ and $\text{rms}(G) = 0.55 \pm 0.01$ for $\beta=4$. In this regime, we found that $\langle G \rangle \leq 1$ which clearly corresponds to the crossover regime. To confirm that the first and second plateaus are indeed in the diffusive and crossover regimes, respectively, we have calculated the localization length ξ of the quasi-1D system (insets of Fig. 1). It is clear that near the first plateau where $W \sim 0.4$ for $\beta=2$ and $W \sim 1$ for $\beta=4$, we have $\xi \gg L$ with L the length of quasi-1D system while near the second plateau, we have $\xi \sim L$ (see insets of Fig. 1).

According to the UCF in the diffusive regime, it is tempting to conclude that this second plateau should correspond to a UCF. However, in making such a claim, one has to answer following questions: (1) is the plateau behavior universal? (2) if it is, whether can it be observed in a wide range of parameters? (3) how is our result compared to the theoretical predictions whenever available? (4) does such a universal behavior exists in high dimensions? In the following, we provide evidences that the plateau indeed corresponds to a UCF.

To answer the first question, we plot $\text{rms}(G)$ vs $\langle G \rangle$ in Fig. 2(a) by eliminating W . The fact that all curves shown in Fig. 1 with different parameters [Fermi energy E , magnetic flux ϕ , and spin orbit interaction (SOI) strength t_{so}] collapse into a single curve for each β strongly indicates that $\text{rms}(G)$ vs $\langle G \rangle$ is universal. To further demonstrate this universal behavior, we have calculated the conductance fluctuation for a quasi-1D system with both magnetic flux and Rashba SOI. Although the Hamiltonian of this system is still unitary, both time-reversal and spin rotation symmetries are broken. According to the diagrammatic perturbation theory,¹² the UCF is reduced by a factor of 2 when SOI is turned on. This is true with or without the magnetic field ($\beta=1$ or 2). From RMT point of view, both systems ($B \neq 0, t_{so}=0$) and ($B \neq 0, t_{so} \neq 0$) are unitary ensembles and obey the same statistics. The fact that energy spectrum for ($B \neq 0, t_{so}=0$) is doubly degenerate accounts for the factor of 2 reduction for the system ($B \neq 0, t_{so} \neq 0$). In Fig. 2(a), we have plotted $\text{rms}(G)$ vs $\langle G \rangle$ for the system with ($B \neq 0, t_{so} \neq 0$). Once again, we see that all data from different parameters collapse into a single curve. If we multiply this curve by a factor of 2, it collapses with the curve of $\beta=2$ [see inset of Fig. 2(a)]. From

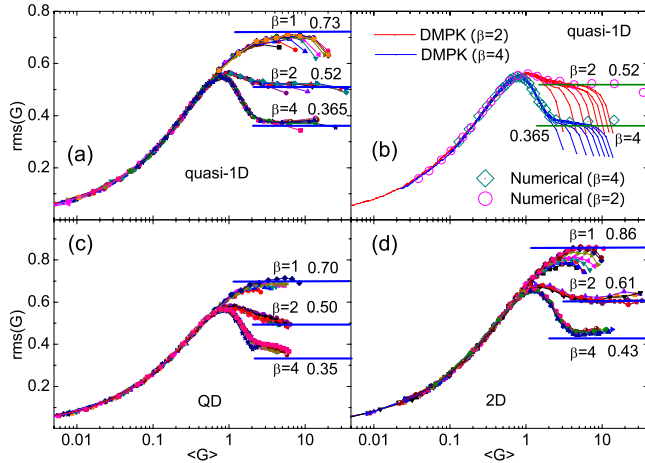


FIG. 2. (Color online) Conductance fluctuation vs average conductance for [(a) and (b)] quasi-1D systems, (c) QD systems, and (d) 2D systems.

Fig. 2(a), we see that in the diffusive regime with $\langle G \rangle > 1$, the long plateau for each β corresponds to the known UCF (marked by solid lines). For $\beta=1$, there is only one plateau. For $\beta=2, 4$, however, a second plateau region is in the neighborhood of $\langle G \rangle \sim 1$. For $\beta=2$, $\text{rms}(G)$ is approximately a constant hence *universal* in the region $\langle G \rangle = (0.6, 1.4)$ while for $\beta=4$, this region is narrower with $\langle G \rangle = (0.7, 0.9)$. Looking at Fig. 2(a), it seems that the second plateau region is narrower than the first one. But if we look at $\text{rms}(G)$ vs W , where W can be controlled experimentally, the crossover region is enlarged since in the crossover regime $\langle G \rangle$ is not very sensitive to W while in the diffusive regime it is the opposite. Indeed, in Fig. 1(f), we do see that the ranges of the first and second plateau regions are comparable. If we fix W and plot $\langle G \rangle$ and $\text{rms}(G)$ vs the length of the system ($s=L/\bar{l}$), the crossover regime is enlarged further. These results are shown in Figs. 3(a) and 3(c) where the symbols represent our numerical result and solid lines correspond to exact solution of DMPK equation (to be discussed below). We see that the

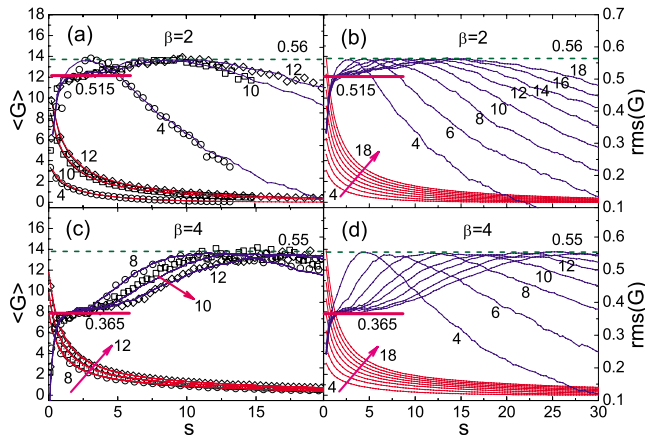


FIG. 3. (Color online) [(a) and (c)] Average conductance and its fluctuation vs s for quasi-1D systems and [(b) and (d)] compared to results of DMPK equation for different $N=4, 6, \dots, 18$. Arrow points the direction of increasing N .

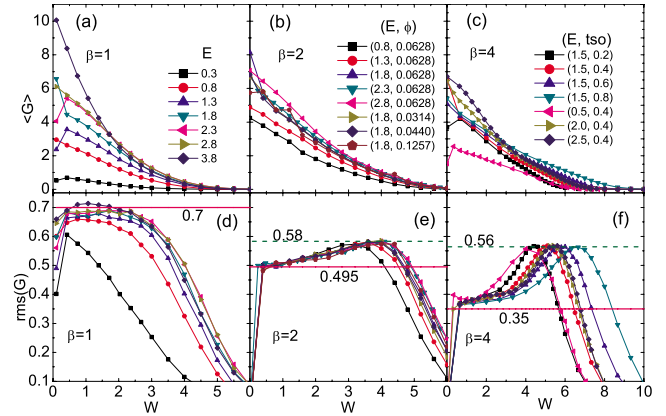


FIG. 4. (Color online) Average conductance and its fluctuation vs W for QD systems with $\beta=1, 2, 4$.

window of the second plateau is much larger than the first one.

Since the statistics of transmission eigenchannels of quasi-1D systems can be described by DMPK equation, we have numerically solved it¹³ for $\beta=2, 4$ and compared our numerical results of tight-binding model to that of DMPK. Figures 3(b) and 3(d) show the numerical solution of DMPK equation for $\beta=2, 4$ with different $N=4, 6, \dots, 18$, where N is the number of transmission channels. Here, $s=L/\bar{l}$, where L is the length of quasi-1D systems and \bar{l} is the average mean-free path.^{2,14} Figure 3 clearly shows that in the diffusive regime where $1 \ll s \ll N$, the first plateau corresponds to the usual UCF and there exists a much wider second plateau in the crossover regime where s and N are comparable to plateau value equal to our identified UCF. Figures 3(a) and 3(c) show the comparison between the results of DMPK and that of quasi-1D tight-binding model. The $\text{rms}(G)$ vs $\langle G \rangle$ of DMPK equation is plotted in Fig. 2(b) where selected data from Fig. 2(a) are also plotted for comparison. The agreement between numerical and theoretical results is clearly seen.

C. Conductance fluctuation in two dimensions

Now we examine the conductance fluctuation for QD systems. In the numerical calculation, the size of QD is $L \times L$ with $L=100$ and the width of the lead $L_0=10$ for $\beta=2, 4$, while for $\beta=1$ we used $L=150$. Figure 4 depicts $\langle G \rangle$ and $\text{rms}(G)$ vs W for $\beta=1, 2, 4$. Each point in Fig. 4 was obtained by averaging 9000 configurations for $\beta=1$ and 20 000 configurations for $\beta=2, 4$. Similar to quasi-1D systems, we see only one plateau region in the diffusive regime for $\beta=1$ with plateau value close to the known UCF value $\text{rms}(G)=0.70$. In addition to the first plateau in the diffusive regime, there exists a second plateau for $\beta=2, 4$ which we identify to be the regime for UCF. The UCF is again in the crossover regime where $\langle G \rangle \sim 1$ with the value $\text{UCF}(\beta=2)=0.58 \pm 0.01$ and $\text{UCF}(\beta=4)=0.56 \pm 0.01$. In Fig. 2(c), we plot $\text{rms}(G)$ vs $\langle G \rangle$. It shows that all curves for each β collapse into a single curve showing universal behaviors. Figures 4(e) and 4(f) show that the universal regime can be quite

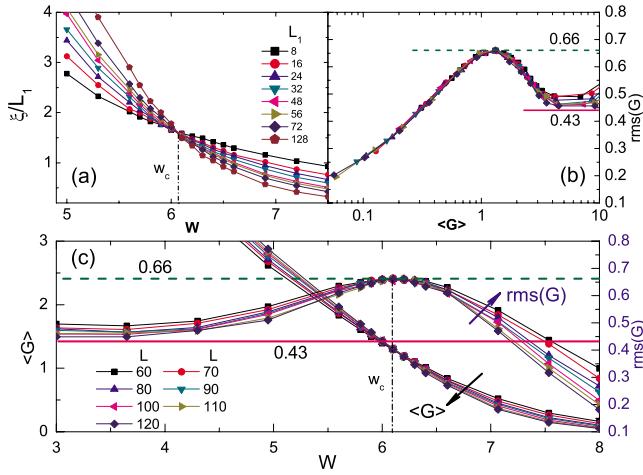


FIG. 5. (Color online) Localization length, average conductance, and conductance fluctuation of 2D symplectic systems for different L with $E=2.3$ and $t_{so}=0.4$. (a) ξ/L_1 vs W . (b) $\text{rms}(G)$ vs $\langle G \rangle$ for different $L=60, 70, \dots, 120$. (c) $\text{rms}(G)$ and $\langle G \rangle$ vs W .

large. Finally, we have also calculated the conductance fluctuation for 2D systems and similar behaviors were found [see Fig. 2(d)].¹⁵ In particular, the values of UCF are found to be $\text{UCF}(\beta=2)=0.68 \pm 0.02$ and $\text{UCF}(\beta=4)=0.66 \pm 0.01$.

Now we provide further evidence of the universal behavior of UCF. In 2D systems, there can be a metal-insulator transition (MIT) for $\beta=2, 4$ but not for $\beta=1$. This somehow coincides with our findings that there is a UCF regime for $\beta=2, 4$ but not for $\beta=1$. To explore this correspondence further, we have calculated the localization length of the 2D system using the transfer-matrix approach.¹⁶ Here we calcu-

late the localization length ξ for quasi-1D systems with fixed length 1 000 000 and different widths L_1 [see Fig. 5(a)]. Figure 5(a) depicts the localization length ξ/L_1 vs disorder strength for $\beta=4$. The intersection of different curves gives an estimate of the critical disorder strength of MIT of the 2D system.¹⁷ Figure 5(a) shows that for an infinite 2D system, there is a MIT around $W_c=6.1$. For a mesoscopic 2D system, the critical region becomes a crossover region around the same W_c and it is in this region where the UCF is found. To see how our UCF evolves with increasing of system size L , we have calculated $\text{rms}(G)$ vs W for finite 2D systems with different sizes $L=50+10n$, where $n=1, 2, \dots, 7$. As shown in Fig. 5(c), for a fixed W that is beyond the crossover regime, e.g., $W=7$, the fluctuation decreases as L increases so that $\text{rms}(G) \rightarrow 0$ at $L \rightarrow \infty$. Importantly, the value of the second plateau (the UCF) does not change with L . In addition, both $\langle G \rangle$ and $\text{rms}(G)$ converge at $W_c=6.1$ for different L . This means that when L goes to infinity, we should have $\text{rms}(G)=c_\beta$ in the vicinity of critical region where c_β is the UCF. This again suggests that the UCF is driven by MIT and is an universal quantity. Finally $\text{rms}(G)$ vs $\langle G \rangle$ is plotted in Fig. 5(b) for different L which shows the universal behavior that is also independent of L . Similar behaviors were also observed for 2D systems with $\beta=2$.¹⁸

D. Universal conductance distribution

We have demonstrated in Fig. 2 that the conductance fluctuation vs average conductance is a universal function from *diffusive to localized regime*. In the following, we will show that the conductance distribution $P(G)$ is also a universal function from *diffusive to localized regime* that depends only

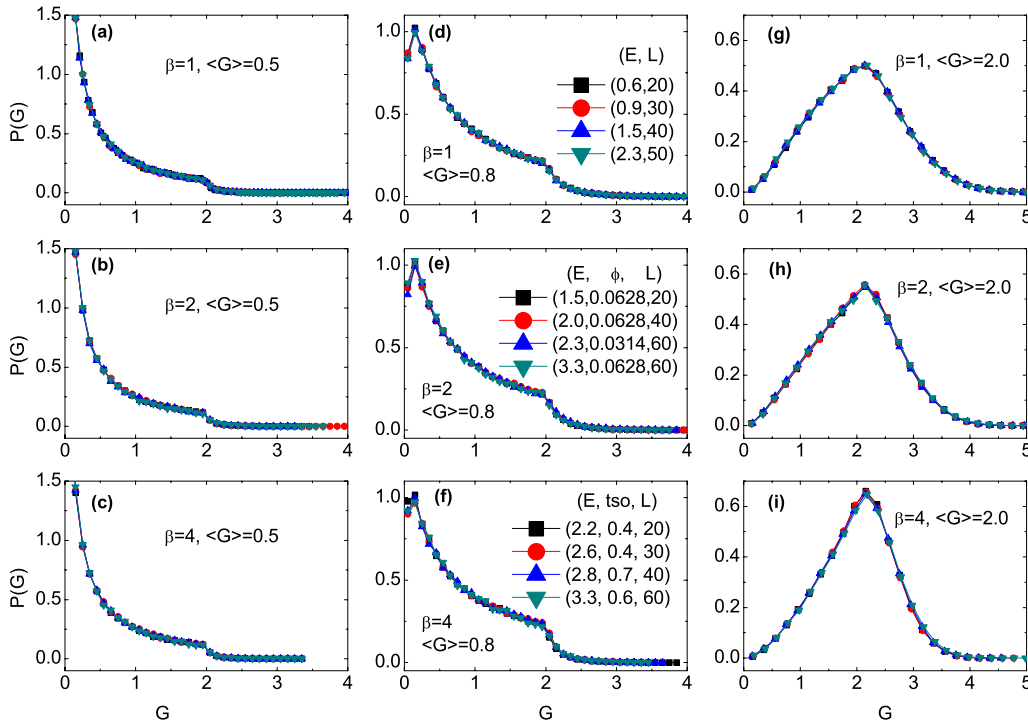


FIG. 6. (Color online) The conductance distribution $P(G)$ vs G at fixed $\langle G \rangle=0.5, 0.8, 2.0$ for 2D systems with $\beta=1, 2, 4$. (a)–(c) correspond to $\langle G \rangle=0.5$ and $\beta=1, 2, 4$. (d)–(f) correspond to $\langle G \rangle=0.8$ and $\beta=1, 2, 4$. (g)–(i) correspond to $\langle G \rangle=2.0$ and $\beta=1, 2, 4$.

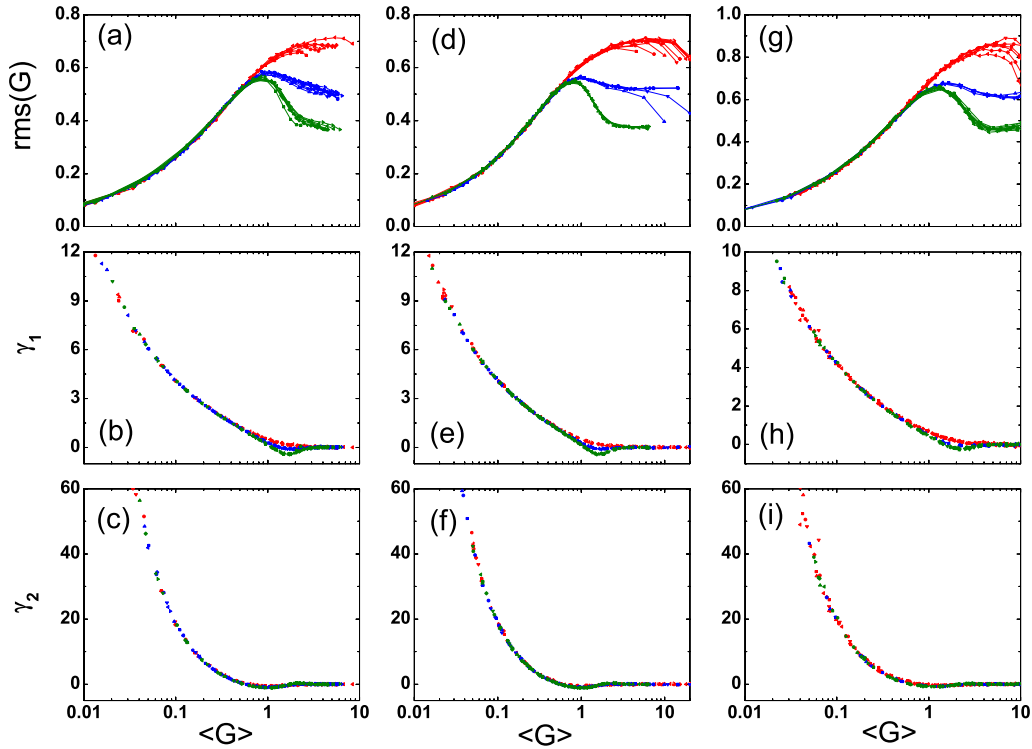


FIG. 7. (Color online) The conductance fluctuation $\text{rms}(G)$, its third and fourth moments γ_1 and γ_2 vs $\langle G \rangle$ for [(a)–(c)] QD systems panel and (d)–(f) quasi-1D systems panel as well as (g)–(i) 2D systems panel with $\beta=1, 2, 4$. In each panel, different symmetries with $=1, 2, 4$ are denoted by symbols with red, blue, and green colors, respectively. Different symbols such as square, circle, star, etc. are used to represent different parameters.

on the average conductance $\langle G \rangle$. To do this, we have plotted $P(G)$ vs G at fixed $\langle G \rangle = 0.2, 0.5, 0.8, 2.0$ for 2D systems with $\beta=1, 2, 4$ using different parameters (see Fig. 6). It can be seen that in each panel, conductance distributions for different system parameters collapse into a single curve. For $\langle G \rangle = 0.5$, conductance distributions in panels (a)–(c) are almost the same for different β which is consistent with the fact that $\text{rms}(G)$ are the same. For $\langle G \rangle = 2.0$, however, the conductance distributions depend on β corresponding to different $\text{rms}(G)$. This clearly suggests that the conductance distribution is a universal function that depends only on average conductance in 2D.

Since it is not practical to plot $P(G)$ vs G for all $\langle G \rangle$, we will show that the second ($\text{rms}(G)$), third (γ_1), and fourth (γ_2) moments¹⁹ of conductance vs $\langle G \rangle$ are universal functions that depend only on dimensionality and symmetry of the system (Fig. 7). Indeed, for QD, quasi-1D, and 2D systems, similar universal features in $\text{rms}(G)$ were also found for γ_1 and γ_2 with different β .²⁰ We see that the conductance fluctuation, the third moment, and fourth moment of conductance γ_1 and γ_2 are universal functions that depend only on $\langle G \rangle$, symmetry, and dimensionality. In Fig. 8(a), we have plotted conductance fluctuation for all systems (QD, quasi-1D, and 2D systems) and all symmetries $\beta=1, 2, 4$ for various parameters. It is interesting to see that in the localized regime with $\langle G \rangle < 0.3$, the conductance fluctuations collapse into a single curve. This suggests that conductance distribution is superuniversal that is independent of dimensionality and symmetry. Indeed, from Fig. 8(b), we have shown the

conductance distributions for all systems and symmetries at $\langle G \rangle = 0.2$ and they give the same conductance distribution. From Fig. 8(c), we see that at $\langle G \rangle = 0.6$, deviation from universal behavior is clearly seen. It is likely that this superuniversal behavior persists in 3D and clearly more work needs to be done to resolve this issue.

In summary, we have carried out extensive simulations on conductance fluctuations of quasi-1D, QD, and 2D mesos-

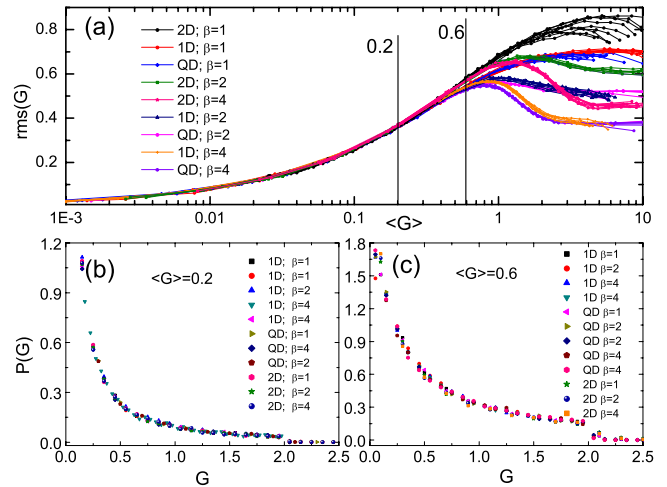


FIG. 8. (Color online) The conductance fluctuation and conductance distribution are depicted for all data from quasi-1D, QD, 2D systems with $=1, 2, 4$. (a) Conductance fluctuation. [(b) and (c)] Conductance distributions at fixed $\langle G \rangle = 0.2$ and 0.6 , respectively.

copic systems for orthogonal, unitary, and symplectic ensembles. Our results show that in addition to the usual UCF in the diffusive regime, there exists a UCF in the crossover regime between metallic and insulating regimes for unitary and symplectic ensembles but not for the orthogonal ensemble. We found that the conductance distribution is a universal function from diffusive to localized regimes that depend only on average conductance, dimensionality, and symmetry of the system. In quasi-1D systems, this universal function agrees with the result from DMPK equation. Our analysis suggests that this UCF is driven by MIT in 2D systems. In the localized regime with $\langle G \rangle < 0.3$, our results

seem to show that the conductance distribution is superuniversal independent of dimensionality and symmetry of the system.

ACKNOWLEDGMENTS

This work was financially supported by a RGC grant (Grant No. HKU 704308P) from the government of HKSAR and LuXin Energy Group. We wish to thank J. R. Shi for providing the code of solving DMPK equation. Computer Centre of The University of Hong Kong is gratefully acknowledged for the high-performance computing assistance.

*jianwang@hkusua.hku.hk

¹L. B. Altshuler, JETP Lett. **41**, 648 (1985); P. A. Lee and A. D. Stone, Phys. Rev. Lett. **55**, 1622 (1985); P. A. Lee, A. D. Stone, and H. Fukuyama, Phys. Rev. B **35**, 1039 (1987).

²C. W. J. Beenakker, Rev. Mod. Phys. **69**, 731 (1997).

³A. Garcia-Martin and J. J. Saenz, Phys. Rev. Lett. **87**, 116603 (2001).

⁴L. S. Froufe-Perez, P. Garcia-Mochales, P. A. Serena, P. A. Mello, and J. J. Sáenz, Phys. Rev. Lett. **89**, 246403 (2002).

⁵M. Ruhlander, P. Markos, and C. M. Soukoulis, Phys. Rev. B **64**, 212202 (2001).

⁶K. A. Muttalib, P. Markos, and P. Wolfle, Phys. Rev. B **72**, 125317 (2005).

⁷K. A. Muttalib and P. Wolfle, Phys. Rev. Lett. **83**, 3013 (1999).

⁸O. N. Dorokhov, JETP Lett. **36**, 318 (1982); P. A. Mello, P. Pereyra, and N. Kumar, Ann. Phys. (N.Y.) **181**, 290 (1988).

⁹Z. Qiao, W. Ren, J. Wang, and H. Guo, Phys. Rev. Lett. **98**, 196402 (2007).

¹⁰W. Ren, Z. Qiao, J. Wang, Q. Sun, and H. Guo, Phys. Rev. Lett. **97**, 066603 (2006).

¹¹J. H. Bardarson, I. Adagideli, and P. Jacquod, Phys. Rev. Lett. **98**, 196601 (2007).

¹²S. C. Feng, Phys. Rev. B **39**, 8722 (1989).

¹³D. Li and J. Shi, Phys. Rev. B **79**, 241303(R) (2009).

¹⁴J. Heinrichs, Phys. Rev. B **76**, 033305 (2007).

¹⁵For 2D systems [in Fig. 2(d)], we have shown data obtained from at least five different sets of parameters for each β .

¹⁶A. MacKinnon and B. Kramer, Phys. Rev. Lett. **47**, 1546 (1981);

Z. Phys. B: Condens. Matter **53**, 1 (1983).

¹⁷Similar analysis has been done. See, for instance, L. Sheng, D. N. Sheng, and C. S. Ting, Phys. Rev. Lett. **94**, 016602 (2005) and P. Markos and L. Schweitzer, J. Phys. A **39**, 3221 (2006).

¹⁸The purpose of this work is not to investigate the critical behavior of MIT. For detailed analysis of MIT in 2D, see P. Markos, Acta Phys. Slov. **56**, 561 (2006) and F. Evers and A. D. Mirlin, Rev. Mod. Phys. **80**, 1355 (2008).

¹⁹W. Ren, J. Wang, and Z. Ma, Phys. Rev. B **72**, 195407 (2005).

²⁰The following parameters are used in Fig. 7: (A) QD systems. (1) When $\beta=1$, $E=0.8, 1.3, 1.8, 2.4, 2.8, 3.8$ with the system size ($L_0=10$, $L=150$). (2) For $\beta=2$, $(\phi, E)=(0.005, 1.8), (0.007, 1.8), (0.01, 0.8), (0.01, 1.3), (0.01, 1.8), (0.01, 2.3), (0.01, 2.8), (0.02, 1.8)$ with the system size ($L_0=10$, $L=150$). (3) For $\beta=4$, $(E, t_{so})=(0.5, 0.4), (1.5, 0.2), (1.5, 0.4), (1.5, 0.6), (1.5, 0.8), (2.0, 0.4), (2.5, 0.4)$ with the system size ($L_0=10$, $L=100$). (B) Quasi-1D systems. (1) For $\beta=1$, $E=0.2, 0.4, 0.6, 0.9, 1.2, 1.5, 1.8, 2.1, 2.4, 2.7, 3.0, 3.3$ with system size 40×2000 . (2) for $\beta=2$, $(\phi, E)=(0.0005, 3.8), (0.005, 3.8), (0.01, 0.8), (0.01, 1.8), (0.01, 2.8), (0.01, 3.8)$ with system size 40×2000 . (3) For $\beta=4$, $(E, t_{so})=(2.5, 0.2), (2.5, 0.4), (0.5, 0.6), (1.5, 0.6), (2.5, 0.6), (3.5, 0.6), (2.5, 0.8)$ with the system size 40×800 . (C) 2D systems. (1) When $\beta=1$, $E=2.15, 2.3, 2.5, 1.54, 1.85$ for $L=100$. (2) When $\beta=2$, $(\phi, E)=(0.01, 1.8), (0.005, 2.0), (0.01, 2.8), (0.007, 1.5)$ for $L=100$. (3) When $\beta=4$, $(E, t_{so})=(3.3, 0.2), (0.8, 0.4), (1.8, 0.4), (2.3, 0.4), (3.3, 0.4), (3.3, 0.6)$ for $L=100$, $(E, t_{so})=(2.3, 0.4)$ for $L=110$, and $(E, t_{so})=(2.3, 0.4)$ for $L=120$.